ACS APPLIED MATERIALS & INTERFACES

RESEARCH ARTICLE

www.acsami.org

Highly Efficient Decomposition of Organic Dye by Aqueous-Solid Phase Transfer and In Situ Photocatalysis Using Hierarchical Copper Phthalocyanine Hollow Spheres

Mingyi Zhang,[†] Changlu Shao,[*,†] Zengcai Guo,[‡] Zhenyi Zhang,[†] Jingbo Mu,[‡] Peng Zhang,[†] Tieping Cao,[†] and Yichun Liu[†]

[†]Center for Advanced Optoelectronic Functional Materials Research, and Key Laboratory of UV Light-Emitting Materials and Technology of Ministry of Education, and [‡]Department of Chemistry, Northeast Normal University, 5268 Renmin Street, Changchun 130024, People's Republic of China

Supporting Information

ABSTRACT: The hierarchical tetranitro copper phthalocyanine (TNCuPc) hollow spheres were fabricated by a simple solvothermal method. The formation mechanism was proposed based on the evolution of morphology as a function of solvothermal time, which involved the initial formation of nanoparticles followed by their self-aggregation to microspheres and transformation into hierarchical hollow spheres by Ostwald ripening. Furthermore, the hierarchical TNCuPc hollow spheres exhibited high adsorption capacity and excellent simultaneously visible-light-driven photocatalytic performance for Rhodamine B (RB) under visible light. A possible mechanism for the "aqueous-solid phase transfer and in situ photocatalysis" was suggested. Repetitive tests showed that the hierarchical TNCuPc hollow spheres maintained high catalytic activity over several cycles, and it had a better regeneration capability under mild conditions.

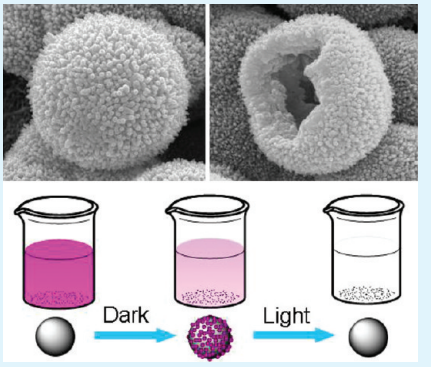

KEYWORDS: phthalocyanine, hierarchical, hollow spheres, solvothermal, adsorption, photocatalysis

1. INTRODUCTION

Organic compounds are widely dispersed and likely to occur as environmental hazards in water. Among different organic pollutants, dyes have been designated as priority pollutants by many countries, because of their acute toxicity and long persistence.[1] Thus, they must be degraded to below environmentally accepted levels before safe disposal to public health. Various technologies, such as biodegradation, adsorption, catalytic wet oxidation, advanced oxidation processes (AOPs), etc., have been conventionally used for dyes treatment.[2−7] Among these methods, adsorption techniques and photocatalytic degradation have been extensively investigated. Adsorption techniques have potential for removing organics from water, because of their high efficiency and ability to separate a wide range of chemical compounds. On the other hand, photocatalytic degradation has received much attention as an alternative method in the removal of environmental pollutants in aqueous as well as gaseous media. Anatase-type TiO_2 has been proven as environmental friendly catalysts, because of its capability to decompose the different organic and inorganic pollutants.[8−11]

Considering the effectiveness of adsorption methods and these ground-breaking results of TiO_2 photocatalytic degradation, some groups designed an efficient supported photocatalyst system, which combines adsorbent material and TiO_2 photocatalyst together.[12−14] In those works, the efficiency of TiO_2 photocatalytic degradation could be enhanced via the anchoring of photocatalysts on suitable supports, particularly those with a large surface area. The adsorption of pollutants on high-surface-area supports, e.g., cellulosic fiber and active carbons, increases their concentration around supported photocatalysts; their diffusion into photocatalysts thereby promotes the photocatalytic process. However, there were some deficiencies in this system. First, the supports may negatively affect catalyst utilization, especially in photocatalysis systems, where some of the active sites were hidden inside the support and were not accessible by the light.[15] Second, for the TiO_2 photocatalysts, a major handicap is its rather large optical band gap (3.2 eV for the anatase phase), which means it could only be activated by ultraviolet (UV) light (λ < 400 nm).[16] According to the solar spectrum, UV light accounts for only a small fraction (4%) of the incoming solar energy, whereas visible light comprises as much as 43%. All the analysis above implied that it was highly desirable to integrate the advantages of both high adsorption capacity and visible-light-driven photocatalytic activity into one compound.

Phthalocyanines, especially those metal phthalocyanines, could be referred to as attractive alternatives for the visible-light-induced photocatalytic decomposition of dye compounds.[17−21] Photoactivity of phthalocyanines arises from their ability to produce the highly active $^1O_2$ singlet oxygen species upon photon

Received: April 5, 2011
Accepted: June 16, 2011
Published: June 16, 2011

flux absorption in either UV or visible parts of the spectrum. This singlet oxygen is formed during the extinction mechanism of the excited triplet state, following its collision with molecular O_2. Details on this mechanism are given elsewhere.[22,23] In addition, besides this property, phthalocyanines revealed very good photostability, negligible toxicity, and high thermal and chemical stability. More importantly, in our previous work, we found that nanoscale phthalocyanines reveal very good adsorption for the organic dye.[24] Because of the above advantages, phthalocyanines might be seriously considered as practically available photocatalysts that have high adsorption capacity and in situ photocatalytic activity for the treatment of water contaminated with many organic dyes.

Based on the above considerations, here, we attempted to construct an "aqueous−solid phase transfer and in situ photocatalysis" system, to solve the problems of supported photocatalyst systems. In this system, azo dyes such as Rhodamine B (RB) could be quickly adsorbed onto/into the photocatalysts from aqueous solution and decomposed in situ simultaneously in the presence of visible light. After a careful inspection of the feasibility and photocatalytic efficiency of the metal phthalocyanines, tetranitro copper phthalocyanine (TNCuPc) hierarchical hollow spheres were chosen as tested materials and fabricated via a solvothermal method for the first time. The photodegradation of RB was employed to evaluate the adsorption capacity and photocatalytic activities of TNCuPc hierarchical hollow spheres under visible-light irradiation. As a result, the hierarchical hollow-sphere nanostructures exhibited high adsorption capacity and excellent simultaneously in situ visible-light-driven photocatalytic performance. The formation mechanism of the hierarchical hollow sphere and the effects of reaction time were also investigated. Moreover, such simple and versatile strategy can provide a general way to fabricate other phthalocyanine nanostructures, such as tetranitro cobalt phthalocyanine (TNCoPc) nanballs, tetranitro nickel phthalocyanine (TNNiPc) nanorods.

2. EXPERIMENTAL SECTION

2.1. Preparation of Hierarchical TNCuPc Hollow Spheres. The synthesis and chemical structure of TNCuPc were shown in Figure S1 in the Supporting Information. In a typical experiment, 4-nitrophthalonitrile (0.100 mmol), $Cu(Ac)_2 \cdot 2H_2O$ (0.025 mmol) and ammonium molybdate (1 mg) were put into a Teflon-lined stainless steel autoclave with a capacity of 25 mL, containing 20 mL of ethylene glycol solution. The mixture was then stirred to form a milk-like suspension, which was then sealed and solvothermally treated at 160 °C for 20 h. The autoclave then was cooled to room temperature. The obtained sample was washed with deionized water and ethanol to remove any ionic residual, then dried in an oven at 80 °C for 4 h.

2.2. Characterization. Field-emission scanning electron microscopy (FESEM) (Model XL-30 ESEM FEG, Micro FEI Philips) was used to characterize the morphologies of the products. An energy-dispersive X-ray (EDX) spectroscopy system, which was attached to scanning electron microscopy (SEM) equipment was used to analyze the composition of the samples. X-ray diffraction (XRD) patterns of the samples were recorded on a Rigaku Model D/max-2500 X-ray diffractometer. Fourier transform infrared (FT-IR) spectra were obtained using a Magna Model 560 FT-IR spectrometer with a resolution of 1 cm^{-1}. X-ray photoelectron spectroscopy (XPS) was performed on a VG-ESCALAB Model LKII instrument with Mg KR ADES ($h\nu$ = 1253.6 eV) source at a residual gas pressure of $<1 \times 10^{-8}$ Pa. Surface areas were calculated using the Brunauer−Emmett−Teller (BET) equation. The ultraviolet-visible (UV−vis) diffuse reflectance (DR) spectroscopy of the samples were recorded on a Cary Model 500 UV-vis-NIR spectrophotometer.

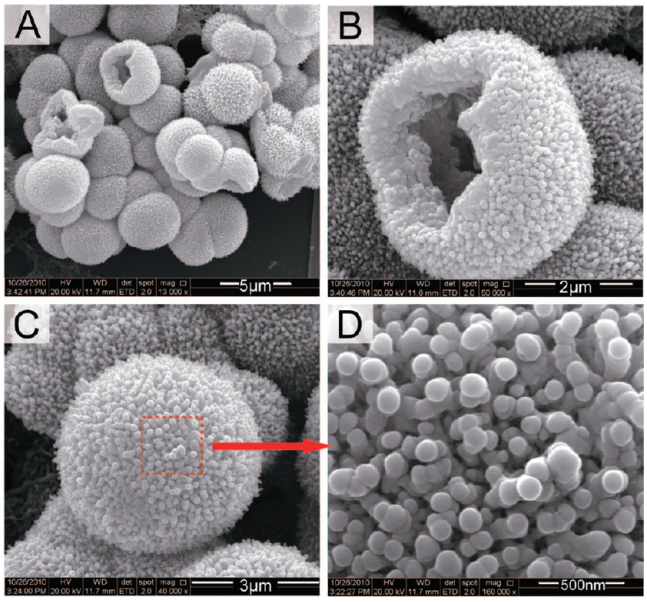

Figure 1. (A) Low-magnification SEM image of the TNCuPc hierarchical hollow spheres. (B,C) High-magnification SEM image of the TNCuPc hierarchical hollow spheres. (D) High-magnification view of the area highlighted in panel C.

2.3. Photocatalytic Test. The photoreactor was designed with an internal xenon lamp (XHA, 150 W) equipped with a cutoff glass filter transmitting light at a wavelength of $\lambda > 400$ nm, surrounded by a water-cooling quartz jacket to cool the lamp, with 100 mL of the RB solution with an initial concentration of 10 mg L^{-1} in the presence of a solid catalyst (0.05 g). The solution was stirred in darkness for 30 min to obtain a good dispersion and reach adsorption−desorption equilibrium between the organic molecules and the catalyst surface. Decreases in the concentrations of dyes were analyzed by a Cary Model 500 UV-vis-NIR spectrophotometer at λ = 553 nm. At given intervals of illumination, 3-mL aliquots were collected from the suspension and immediately centrifuged; the concentration of RB after illumination was determined at λ = 553 nm using a UV-vis spectrophotometer.

3. RESULTS AND DISCUSSION

3.1. Morphology and Structure of the Hierarchical TNCuPc Hollow Spheres. Figure 1 showed the typical SEM images of the hierarchical TNCuPc hollow spheres. Figure 1A was a low-magnification SEM image of the as-prepared product, from which numerous uniformly sized spheres with an average diameter of 2−3 μm could be clearly observed. Moreover, no other morphologies could be detected, indicating a high yield of the product with the spherical morphology. The high-magnification SEM image of an individual broken sphere is shown in Figure 1B. The broken sphere had a bowl-like shape and the wall thicknesses of the sphere are 500−700 nm, indicating that the spheres had a hollow structure. A typical microsphere is shown in the magnified SEM image in Figure 1C, and more details marked with a rectangle in Figure 1C are shown in Figure 1D, which demonstrated that the exterior of each hollow sphere were composed of abundant randomly assembled nanospheres with an average diameter of ∼50 nm. Meanwhile, Figure S2 in the Supporting Information showed the EDX spectrum of the

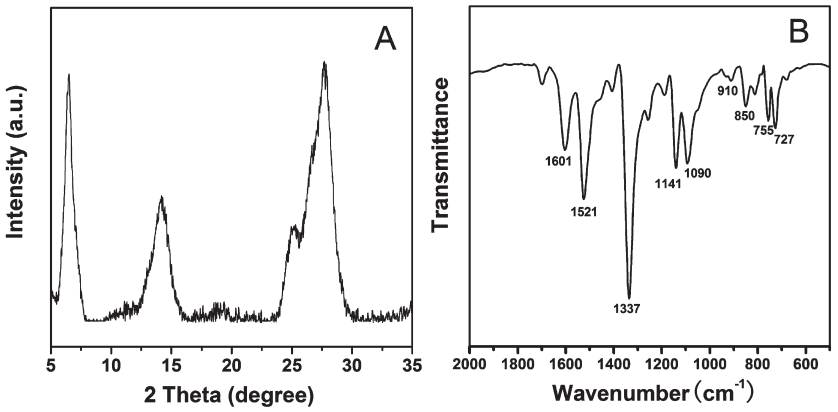

Figure 2. (A) XRD patterns and (B) FT-IR spectra of the TNCuPc hierarchical hollow spheres.

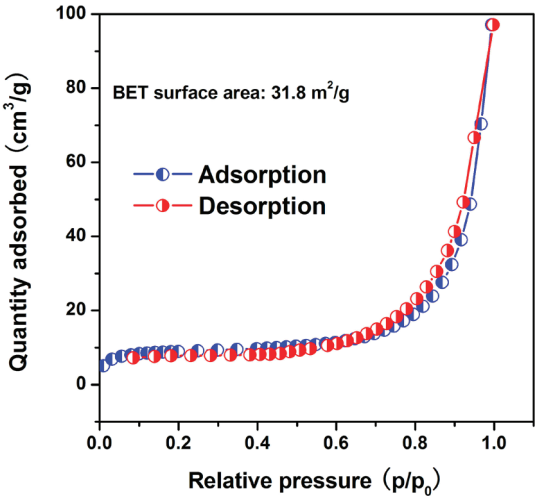

Figure 3. N_2 adsorption−desorption isotherm curves of the TNCuPc hierarchical hollow spheres.

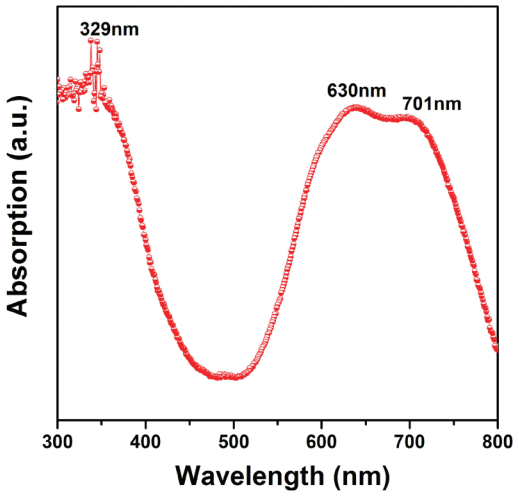

Figure 4. UV−vis diffuse reflectance spectrum of the TNCuPc hierarchical hollow spheres.

hierarchical TNCuPc hollow spheres. It indicates that elemental carbom, nitrogen, oxygen, and copper exists in the hierarchical TNCuPc hollow spheres.

Figure 2 shows the X-ray diffraction (XRD) pattern and FT-IR spectrum of the hierarchical hollow spheres. As observed in Figure 2A, four main reflection peaks appeared, at 2θ = 6.4°, 13.8°, 24.7°, and 27.5°, which could be indexed to the diffraction peaks of TNCuPc.[25] From Figure 2B, it is observed that the hierarchical TNCuPc hollow spheres showed several absorption peaks at ∼727, 755, 910, 1090, 1141, and 1605 cm^{-1}, which might be assigned to phthalocyanine skeletal and metal−ligand vibrations.[26,27] The other absorption peaks at 1521, 1337, and 850 cm^{-1} might be respectively assigned to the asymmetric N−O stretching, symmetric N−O stretching, and C-NO_2 stretching, because of the nitro groups present in the structure of the TNCuPc molecule.[25] In addition, the chemical composition and purity of the hierarchical TNCuPc hollow spheres was studied using X-ray photoelectron spectroscopy (XPS) analysis. The fully scanned spectra in Figure S3A in the Supporting Information demonstrated that elemental carbon, nitrogen, oxygen, and copper existed in the hierarchical TNCuPc hollow spheres. As observed in Figure S3B in the Supporting Information, there were two symmetric peaks in the Cu 2p region. The peak centered at 935.1 eV corresponded to Cu $2p_{3/2}$, and another one centered at 955.2 eV was assigned to Cu $2p_{1/2}$, indicating a normal state of Cu^{2+} in the hierarchical TNCuPc hollow spheres. All of the results above confirmed the formation of the target product of TNCuPc.

The surface structures of the hierarchical TNCuPc hollow spheres were analyzed by nitrogen sorption isotherm techniques. Figure 3 presented the nitrogen adsorption−desorption isotherms of the above TNCuPc hollow spheres. As observed in Figure 3, the BET surface areas of the prepared hierarchical TNCuPc hollow spheres are 31.8 $m^2 g^{-1}$. The larger BET surface area was attributed to the surface hierarchical nanostructures of the hierarchical hollow spheres. The larger BET surface area and hierarchical hollow structure could have facilitated more-efficient contact of hierarchical TNCuPc hollow spheres with organic contaminants and thus improved its photocatalytic activity.

The optical absorption of the hierarchical TNCuPc hollow spheres was conducted with a UV−vis absorption spectrometer. As shown in Figure 4, the hierarchical TNCuPc hollow spheres exhibited absorption bands in the wavelengths of 600−750 nm, which might be attributed to the Q-band of TNCuPc.[28] The Q-band corresponds to excitation between the ground-state a_{1u} (π) highest occupied molecular orbital (HOMO) to the e_g (π^*) lowest unoccupied molecular orbital (LUMO). Furthermore, two splitting absorption bands were observed at ∼630 and

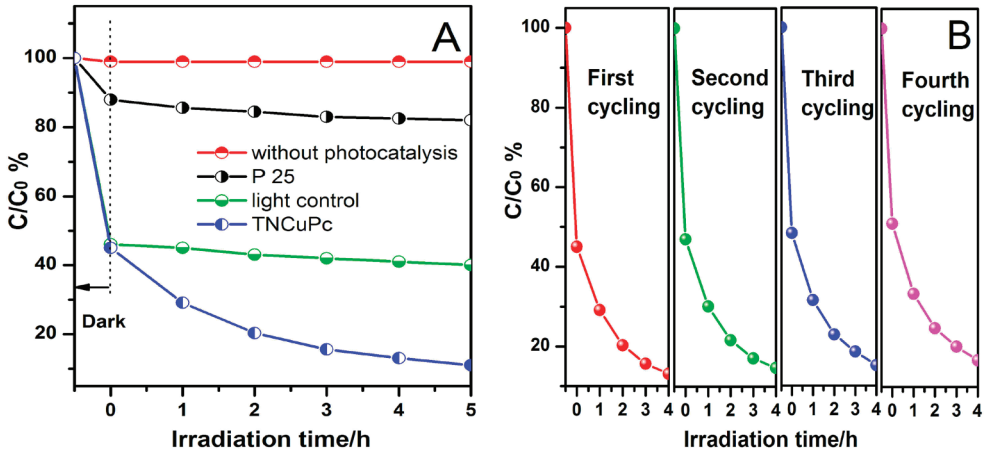

Figure 5. (A) Adsorption and photocatalytic degradation of RB by different photocatalysts with the same weight under visible-light irradiation. (B) Photocatalytic activity of the sample for RB degradation with three times of cycling uses.

710 nm, which is likely due to the vibronic coupling in the excited state.[29−31] The band at 300−450 nm belonged to the typical Soret-band (B-band) absorption of phthalocyanine. Gouterman suggested that the B (Soret) band is due to the $a_{2u}-e_g$ transition.[32] The phthalocyanines in the solid state behave as *p*-type semiconductors, characterized by a band-gap energy of ~2 eV.[33−36] This indicated that the hierarchical TNCuPc hollow spheres had a suitable band gap for photocatalytic decomposition of organic contaminants under visible-light irradiation.

3.2. Adsorption Capacity and Photocatalytic Properties. The photocatalytic activities of the hierarchical TNCuPc hollow spheres were evaluated by the degradation of RB in aqueous solution under visible-light irradiation. Before studying and comparing the activities of the hierarchical TNCuPc hollow spheres, the bleaching of RB in the absence of any catalysts was first examined. As shown in Figure 5A, RB degradation without a photocatalyst was also performed, and the results demonstrated that the degradation of RB was very slow in the absence of a photocatalyst under visible-light irradiation. Next, the photocatalytic activities of the Degussa-P25 was studied. It can be seen that the Degussa-P25 had no photocatalytic activity under the visible light, except decent adsorption for RB, which could be attributed to the high specific surface area of the samples. As shown in Figure 5A, in the presence of hierarchical TNCuPc hollow spheres but in darkness, the removal rate of RB was ~56% within 30 min. Almost no change occurred during the next 270 min, which was attributed to the good adsorption capacity of TNCuPc, while the adsorption of RB was close to saturation by the end of the initial 30 min. It seems very important to consider whether photocatalysis could still happen effectively after the adsorption of RB to hierarchical TNCuPc hollow spheres reached equilibrium. Indeed, ~91% of the RB was degraded under identical conditions, but under irradiation with visible light. This demonstrated that the hierarchical hollow-sphere nanostructures exhibited high adsorption capacity and excellent simultaneously in situ visible-light-driven photocatalytic performance.

Moreover, the regeneration capability of the hierarchical TNCuPc hollow spheres was examined for degradation of dye during a four-cycle experiment, which was very important for the hierarchical TNCuPc hollow spheres to apply in environmental technology. As shown in Figure 5B, each experiment was carried out under identical conditions; after a four-cycle experiment, the photocatalytic activity of the hierarchical TNCuPc hollow spheres remained almost unchanged. It was indicated that the hierarchical TNCuPc hollow spheres displayed an efficient photoactivity for the degradation of organic pollutants under visible-light irradiation and could easily be separated for reuse.

Based on the above results and the earlier reports on the supported catalyst systems,[12,37,38] a proposed mechanism of "aqueous−solid phase transfer and in situ photocatalysis" of RB with the TNCuPc hierarchical nanostructures was elucidated as follows. In the initial stage of degradation RB solution, the color of the reaction solution did not change. When hierarchical TNCuPc hollow spheres were added into the RB dye solution, the color of the RB solution changed from pink to light pink. Meanwhile, the major absorption peaks of RB at ~553 nm diminished gradually under visible-light irradiation in the presence of hierarchical TNCuPc hollow spheres, which indicated the adsorption of the RB dye on the photocatalyst (see Figure S4 in the Supporting Information). Finally, since the pink dye on the catalyst decomposed eventually over time, the color of the RB solution changed to a transparent color. It is believed that the relationship of hierarchical TNCuPc hollow spheres to dyes involved van der Waals forces and hydrogen bonds, resulting in an anchor effect of dye molecule onto/into the hierarchical TNCuPc hollow spheres. On the other hand, the dyes anchored onto/into the hierarchical TNCuPc hollow spheres can therefore be degraded rapidly and effectively in situ at the surface and interior of hierarchical TNCuPc hollow spheres. Because of the high affinity of the hierarchical TNCuPc hollow spheres toward dyes and the concentration difference between these two phases, the decomposed dyes could be replenished continuously with dyes in the aqueous phase until complete depletion. However, in the absence of visible light in the dye solution, the color of the RB solution kept its light pink color, indicating that the adsorption occurred, but the photocatalysis did not.

3.3. Formation Mechanism of the Hierarchical TNCuPc Hollow Spheres. To well understand the formation mechanism of the hierarchical TNCuPc hollow sphere, products formed at different solvothermal reaction times were examined via SEM. Figures 6A−D show SEM images of the products obtained at different reaction stages, clearly reflecting the morphology evolution process of the products. The structure and morphology of the precursor were found to be largely dependent on the

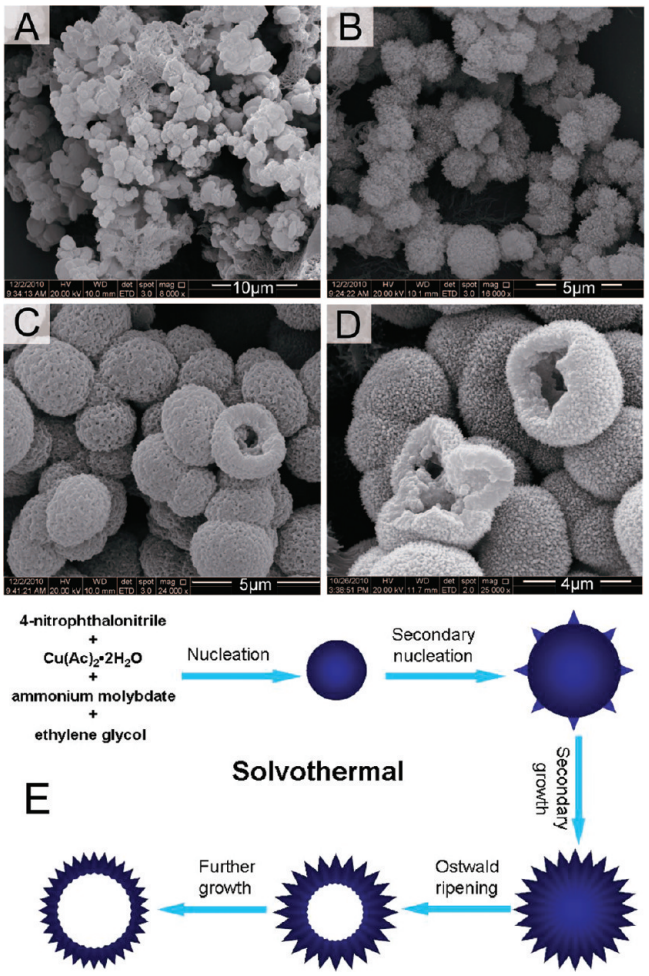

Figure 6. Time-dependent morphological evolution of the TNCuPc samples obtained for different solvothermal times: (A) 20 min, (B) 1 h, (C) 8 h, and (D) 20 h. Panel E shows the formation mechanism of a TNCuPc hierarchical hollow sphere.

solvothermal reaction time. As shown in Figure 6A, only nanoparticles with a diameter of ~500 nm were obtained when the solvothermal reaction time is 20 min. When the solvothermal reaction time is extended to 1 h, microspheres with a diameter of ~1 μm gradually appeared, accompanying the small nanoparticles (see Figure 6B). When the solvothermal reaction time was prolonged to 8 h, hierarchical solid hollow microspheres were obtained on a large scale, as shown in Figure 6C. However, these hierarchical solid microspheres are only the intermediate stage. The internal part of the solid microsphere gradually reaggregated. Finally, the hierarchical TNCuPc hollow spheres were obtained after the solvothermal reaction was carried out for 20 h (see Figure 6D).

Based on the above experimental results, the possible growth pattern and formation mechanism of the hierarchical TNCuPc hollow spheres are shown in Figure 6E. During the initial stage of the solvothermal process, because of the high temperature and high pressure, TNCuPc nanoparticles were produced and tend to assemble into spherical agglomerates driven by reducing the surface energy of the nanoparticles. Subsequently, the Cu^{2+} and 4-nitrophthalonitrile in the solution prefer transferred onto the surface of the nanoparticles and nucleated on the small protuberances, which provided many high-energy sites for the growth of nanostructures. These aggregated nanoparticles then would further serve as seeds to grow into secondary nanostructures for the hierarchical TNCuPc hollow spheres. As the solvothermal time was prolonged, the internal part of the solid microsphere gradually dissolved and reaggregated. Finally, the hierarchical TNCuPc hollow spheres are formed, because of mass diffusion and Ostwald ripening.

Last but not least, the simple experimental procedure for the hierarchical TNCuPc hollow spheres makes this method quite simple, environmentally benign, and cost-effective for the synthesis of other metal phthalocyanines for various applications. Figure S5 in the Supporting Information shows the SEM image of two nanostructures prepared by the similar solvothermal method. It can be seen that various nanostructures, such as TNCoPc nanoballs and TNNiPc nanorods, can be successfully fabricated, demonstrating the generality of the present method. We believe such method may open new pathways to designing other organic nanostructures for potential applications such as use in catalysis and opto-electronic devices. Our related work is in progress and will be published later.

CONCLUSIONS

In summary, by using a solvothermal process, the TNCuPc hierarchical hollow spheres were successfully fabricated. The formation mechanism and the effects of reaction time were also investigated. Furthermore, the hierarchical TNCuPc hollow spheres exhibited not only high adsorption capacity, but also excellent photocatalytic activities for RB under visible light. A possible mechanism for the "phase transfer and in situ photocatalysis" was suggested. Also, it is expected that the TNCuPc hierarchical hollow spheres with high photocatalytic activity will greatly promote their industrial application to eliminate the organic pollutants from wastewater.

ASSOCIATED CONTENT

Supporting Information. This material is available free of charge via the Internet at http://pubs.acs.org.

AUTHOR INFORMATION

Corresponding Author

*Tel.: 8643185098803. E-mail: clshao@nenu.edu.cn.

ACKNOWLEDGMENT

The present work is supported financially by the National Natural Science Foundation of China (Nos. 50572014 and 50972027) and the Program for New Century Excellent Talents in University (No. NCET-05-0322).

REFERENCES

(1) Correia, V. M.; Stephenson, T.; Judd, S. *J. Environ. Technol.* **1994**, *15*, 917.

(2) Vandevivere, P. C.; Bianchi, R.; Verstraete, W. *J. Chem. Technol. Biotechnol.* **1998**, *72*, 289.

(3) Legrini, O.; Oliveros, E.; Braun, A. M. *Chem. Rev.* **1993**, *93*, 671.

(4) Sevimli, M. F.; Sarikaya, H. Z. *J. Chem. Technol. Biotechnol.* **2002**, *77*, 842.

(5) Fernandez, J.; Bandara, J.; Lopez, A.; Buffat, Ph.; Kiwi, J. *Langmuir* **1999**, *15*, 185.

(6) Parra, S.; Guasaquillo, I.; Enea, O.; Mielczarski, E.; Mielczarki, J.; Albers, P.; Kiwi-Minsker, L.; Kiwi, J. *J. Phys. Chem. B* **2003**, *107*, 7026.
(7) Liang, X.; Fu, D.; Liu, R.; Zhang, Q.; Zhang, T. Y.; Hu, X. *Angew. Chem., Int. Ed.* **2005**, *44*, 5520.
(8) Konstantinou, I. K.; Albanis, T. A. *Appl. Catal., B* **2004**, *49*, 1.
(9) Fujishima, A.; Rao, T. N.; Tryk, D. A. *J. Photochem. Photobiol. C: Photochem. Rev.* **2000**, *1*, 1.
(10) Kamat, P. V. *Chem. Rev.* **1993**, *93*, 267.
(11) Hoffmann, M. R.; Martin, S. T.; Choi, W.; Bahnemann, D. W. *Chem. Rev.* **1995**, *95*, 69.
(12) Hsu, Y. C.; Lin, H. C.; Lue, C. W.; Liao, Y. T.; Yang, C. M. *Appl. Catal., B* **2009**, *89*, 309.
(13) Inagaki, M.; Kojin, F.; Tryba, B.; Toyoda, M. *Carbon* **2005**, *43*, 1652.
(14) Inagaki, M.; Kobayashi, S.; Kojin, F.; Tanaka, N.; Morishita, T.; Tryba, B. *Carbon* **2004**, *42*, 3153.
(15) Tasbihi, M.; Ngah, C. R.; Aziz, N.; Mansor, A.; Abdullah, A. Z.; Teong, L. K.; Mohamed, A. R. *Ind. Eng. Chem. Res.* **2007**, *46*, 9006.
(16) Linsebigler, A.; Lu, G.; Yates, J. T. *Chem. Rev.* **1995**, *95*, 735.
(17) Guo, Z. C.; Chen, B.; Zhang, M. Y.; Mu, J. B.; Shao, C. L.; Liu, Y. C. *J. Colloid Interface Sci.* **2010**, *348*, 37.
(18) Marais, E.; Klein, R.; Antunes, E.; Nyokong, T. *J. Mol. Catal. A: Chem.* **2007**, *261*, 36.
(19) Palmisano, G.; Gutiérrez, M. C.; Ferrer, M. L.; Gil-Luna, M. D.; Augugliaro, V.; Yurdakal, S.; Pagliaro, M. *J. Phys. Chem. C* **2008**, *112*, 2667.
(20) Mackintosh, H. J.; Budd, P. M.; McKeown, N. B. *J. Mater. Chem.* **2008**, *18*, 573.
(21) Makhseed, S.; Al-Kharafi, F.; Samuel, J.; Ateya, B. *Catal. Commun.* **2009**, *10*, 1284.
(22) Chauke, V.; Nyokong, T. *J. Mol. Catal. A: Chem.* **2008**, *289*, 9.
(23) Sehlotho, N.; Nyokong, T. *J. Mol. Catal. A: Chem.* **2004**, *219*, 201.
(24) Zhang, M. Y.; Shao, C. L.; Guo, Z. C.; Zhang, Z. Y.; Mu, J. B.; Cao, T. P.; Liu, Y. C. *ACS Appl. Mater. Interfaces* **2011**, *3*, 369.
(25) Rajić, N. Z.; Stojaković, D. R. *J. Coord. Chem.* **1989**, *19*, 295.
(26) Seoudi, R.; El-Bahy, G. S.; El Sayed, Z. A. *J. Mol. Struct.* **2005**, *753*, 119.
(27) Kobayashi, T.; Kondo, R.; Nakajima, S. J. *Spectrochim. Acta* **1970**, *26A*, 1305.
(28) Edwards, L.; Gouterman, M. *J. Mol. Spectrosc.* **1970**, *33*, 292.
(29) Nozawa, T. *Biochim. Biophys. Acta* **1980**, *626*, 282.
(30) Nykong, T.; Gasyna, Z.; Stillman, M. J. *Inorg. Chem.* **1987**, *26*, 1087.
(31) VanCott, T. C.; Rose, J. L.; Misener, G. C.; Williamson, B. E.; Schrimpf, A. E.; Boyle, M. E.; Schatz, P. N. *J. Phys. Chem.* **1989**, *93*, 2999.
(32) Edwards, L.; Gouterman, M. *J. Mol. Spectrosc.* **1970**, *33*, 292.
(33) Schlettwein, D.; Kaneko, M.; Yamada, A.; Wöhrle, D.; Jaeger, N. I. *J. Phys. Chem.* **1991**, *95*, 1748.
(34) Tang, C. W. *Appl. Phys. Lett.* **1986**, *48*, 183.
(35) Popovic, Z. D. *Chem. Phys.* **1984**, *86*, 311.
(36) Iliev, V. *J. Photochem. Photobiol. Chem.* **2002**, *151*, 195.
(37) Chen, W. X.; Lu, W. Y.; Yao, Y. Y.; Xu, M. H. *Environ. Sci. Technol.* **2007**, *41*, 6240.
(38) Lu, W. Y.; Chen, W. X.; Li, N.; Xu, M. H.; Yao, Y. Y. *Appl. Catal., B* **2009**, *87*, 146.